

1                   **Exploiting satellite measurements to explore uncertainties in**  
2                   **UK bottom-up NO<sub>x</sub> emission estimates**

3  
4                   Richard J. Pope<sup>1,2</sup>, Rebecca Kelly<sup>1</sup>, Eloise A. Marais<sup>3</sup>, Ailish M. Graham<sup>1</sup>,  
5                   Chris Wilson<sup>1,2</sup>, Jeremy J. Harrison<sup>4,5</sup>, Savio J. A. Moniz<sup>6</sup>, Mohamed Ghalaieny<sup>6</sup>, Steve R.  
6                   Arnold<sup>1</sup> and Martyn P. Chipperfield<sup>1,2</sup>

7  
8                   *1: School of Earth and Environment, University of Leeds, Leeds, UK*

9                   *2: National Centre for Earth Observation, University of Leeds, Leeds, UK*

10                  *3: Department of Geography, University College London, London, UK*

11                  *4: Department of Physics and Astronomy, University of Leicester, Leicester, UK*

12                  *5: National Centre for Earth Observation, University of Leicester, Leicester, UK*

13                  *6: Department for Environment, Food and Rural Affairs, 2 Marsham Street, London, UK*

14  
15  
16                               Resubmitted to *Atmospheric Chemistry and Physics*

17                           Correspondence to: Richard J. Pope (r.j.pope@leeds.ac.uk)

18                   **Abstract**

19   Nitrogen oxides (NO<sub>x</sub>, NO+NO<sub>2</sub>) are potent air pollutants which directly impact on human  
20   health and which aid the formation of other hazardous pollutants such as ozone (O<sub>3</sub>) and  
21   particulate matter. In this study, we use satellite tropospheric column nitrogen dioxide  
22   (TCNO<sub>2</sub>) data to evaluate the spatiotemporal variability and magnitude of the United  
23   Kingdom (UK) bottom-up National Atmospheric Emissions Inventory (NAEI) NO<sub>x</sub> emissions.  
24   Although emissions and TCNO<sub>2</sub> represent different quantities, for UK city sources we find a  
25   spatial correlation of ~0.5 between the NAEI NO<sub>x</sub> emissions and TCNO<sub>2</sub> from the high-  
26   spatial-resolution TROPospheric Monitoring Instrument (TROPOMI), suggesting a good  
27   spatial distribution of emission sources in the inventory. Between 2005 and 2015, the NAEI  
28   total UK NO<sub>x</sub> emissions and long-term TCNO<sub>2</sub> record from the Ozone Monitoring Instrument  
29   (OMI), averaged over England, show annually decreasing trends of 4.4% and 2.2%,  
30   respectively. Top-down NO<sub>x</sub> emissions were derived in this study by applying a simple mass  
31   balance approach to TROPOMI observed downwind NO<sub>2</sub> plumes from city sources. Overall,  
32   these top-down estimates were consistent with the NAEI, but for larger cities such as  
33   London and Manchester the inventory is significantly (>25%) less than the top-down  
34   emissions.

## 1. Introduction

Poor air quality (AQ) can have a substantial impact on human health, increasing risk of ailments such as asthma, cancer, diabetes and heart disease (Royal College of Physicians, 2016). A key air pollutant is nitrogen dioxide ( $\text{NO}_2$ ) which was responsible for approximately 9600 premature deaths from long-term exposure in the UK in 2015 (EEA, 2018).  $\text{NO}_2$  is also a precursor to tropospheric ozone and nitrate aerosol in the UK (DEFRA, 2018a). Legislation (e.g. the EU directive 2008/50/EC Ambient AQ regulation, (DEFRA, 2018a)) is in place to reduce concentrations of  $\text{NO}_2$  and other pollutants. However, many regions in the UK (33 out of 43 in 2019; DEFRA, 2020) still fail to meet the annual mean  $\text{NO}_2$  limit of  $40 \mu\text{g}/\text{m}^3$  (WHO, 2018). To meet the UK's statutory reporting requirements and to help inform policy, Defra uses the National Atmospheric Emissions Inventory (NAEI, 2021). However, like all emission inventories, the NAEI is subject to uncertainties which are difficult to quantify. These uncertainties include unreported sources, diffuse sources such as agriculture, the use of proxy data (e.g. population or housing density data) to distribute emissions and updates to the NAEI methodologies between years (NAEI, 2017). In addition, the NAEI only includes emissions from anthropogenic sources. Spatial verification of the NAEI AQ emissions, until recently (Tsagatakis et al., 2021), has been restricted to comparisons with surface sites, which have limited and disproportional spatial coverage. The NAEI is also used to drive regional models (e.g. the UK Met Office Air Quality in the Unified Model (AQUM, Savage et al., 2013) which provides the official national AQ forecasts), land use regression models (e.g. Wu et al., 2017) and Pollutant Climate Mapping (PCM) models (e.g. Dibbens and Clemens, 2015), where uncertainties in the emissions can then feed into the simulated AQ predictions and resultant public health advisories.

Satellite measurements of tropospheric column  $\text{NO}_2$  ( $\text{TCNO}_2$ ) have frequently been used to derive top-down emissions of nitrogen oxides ( $\text{NO}_x$  = nitric oxide (NO) +  $\text{NO}_2$ ), which can be used to evaluate bottom-up inventories. Some studies have used statistical fitting of observed downwind plumes of  $\text{TCNO}_2$  from anthropogenic sources (e.g. Beirle et al., 2011; Liu et al., 2016; Verstraeten et al., 2018), while others have used complex atmospheric chemistry models deploying approaches such as data assimilation (e.g. Miyazaki et al., 2016), mass balance (Martin et al., 2003) and model sensitivity experiments (e.g. Potts et al., 2021).

While model-derived estimates of  $\text{NO}_x$  emissions (e.g. from data assimilation) are robust, the methodology is computationally expensive and time intensive. Therefore, the statistical fitting to downwind plumes approach is a more achievable approach to derive top-down emissions, especially for government departments and agencies. Beirle et al. (2011) presented one of the first studies to use statistical fitting to downwind plumes for Riyadh, Saudi Arabia. The method was also applied to multiple megacities and compared with the bottom-up Environmental Database for Global Atmospheric Research (EDGAR) emission inventory (version 4.1). Verstraeten et al. (2018) used a similar, but modified, approach of a simple mass balance which assumes that the observed total mass of  $\text{NO}_2$  is a product of the emission rate and the effective lifetime. The assumption is that the removal of  $\text{NO}_2$  can be described by a first-order loss (i.e. the chemical decay of  $\text{NO}_2$  follows an exponential decay function with an e-folding time, and therefore distance from source).

In this study, we use satellite  $\text{TCNO}_2$  records to evaluate the spatial distribution and temporal evolution of the NAEI. In the past, and still presently, this is a challenge given the climatological meteorological conditions (i.e. frequent frontal systems with widespread

precipitation and cloud cover; Pena-Angulo et al., (2020)) experienced in the UK. Frequent cloud cover means that satellite instruments are severely restricted in their ability to retrieve information on trace gases and aerosols through the atmosphere (i.e. retrievals only between the top of atmosphere and cloud top). Therefore, the lack of robust observations makes it more difficult to clearly resolve large emission sources from space. Also, previous sensors (e.g. the Ozone Monitoring Instrument, OMI) have had relatively coarse horizontal spatial resolutions (in the order of 10-100 km) which are larger than most UK emissions sources. However, this work represents the first attempt to derive UK city-scale NO<sub>x</sub> emissions from the new state-of-the-art TROPOspheric Monitoring Instrument (TROPOMI), which has unparalleled spatial resolution in comparison to previous sensors (e.g. OMI). We apply a similar approach to Verstraeten et al. (2018), but determine the background NO<sub>2</sub> value and e-folding distance in different ways, to derive top-down NO<sub>x</sub> emission estimates of UK cities and thereby directly evaluate the NAEI estimates. Therefore, we can derive NO<sub>x</sub> emissions from previously undetectable sources (e.g. Manchester and Birmingham). From here on, we refer to this methodology as the simple mass balance approach (SMBA). The satellite observations used, NAEI and SMBA are described in Section 2, the results presented in Section 3 and our conclusions discussed in Section 4.

## **2. Data and Methods**

### **2.1 NAEI Emissions**

The NAEI is the official UK bottom-up inventory of primary sources of emissions, used for statutory reporting, national air quality policy and driving regional air quality models (NAEI, 2021). The contract to deliver the NAEI is led by a consortium managed by Ricardo Energy and Environment for the UK Department for Business, Energy and Industrial Strategy (BEIS) and the Department for Environment, Food and Rural Affairs (Defra). The NAEI is compiled on an annual basis according to internationally agreed methodologies (EMEP/EEA, 2019), encompassing sectors ranging from transport, industry, through to agriculture and domestic sources (Ricardo Energy and Environment, 2021). Here, we use the NAEI emissions from 2019, which is the most recent version publically available.

### **2.2 Satellite Data**

OMI and TROPOMI are both nadir-viewing instruments on-board the NASA Aura and ESA Sentinel 5 – Precursor (S5P) polar orbiting satellites, respectively, and have local overpass times of 13:30. TROPOMI measures in the ultraviolet-visible (UV-Vis, 270-500 nm), similar to OMI (Boersma et al., 2007), as well as near-infrared (NIR, 675-775 nm) and short-wave infrared (SWIR, 2305-2385 nm) spectral ranges (Veefkind et al., 2012). TROPOMI and OMI have nadir pixel sizes of 3.5 km × 5.5 km (in the UV-Vis, 7.0 km × 7.0 km for other spectral ranges) and 13 km × 24 km, respectively. The OMI (DOMINO version 2 product) and TROPOMI (TM5-MP-DOMINO version 1.2/3x – OFFLINE product) data were downloaded from the Tropospheric Emissions Monitoring Internet Service (TEMIS) for January 2005 to December 2015 and February 2018 to January 2020, respectively. Given the issues with large cloud cover in the UK, we use two years of TROPOMI TCNO<sub>2</sub> data to help increase the spatiotemporal sample size when deriving top-down emissions to evaluate the 2019 NAEI NO<sub>x</sub> emissions. The OMI row anomaly first occurred in 2008 (Torres et al., 2018) and over time has progressively

had a detrimental impact on retrieved TCNO<sub>2</sub>. The study by Pope et al., (2018) successfully used the OMI record to look at long-term trends in UK TCNO<sub>2</sub>. However, after 2015, while still retrieving robust signals over source regions, the row anomaly appears to be substantially artificially enhancing background TCNO<sub>2</sub>. Therefore, as we consider regional trends in TCNO<sub>2</sub> in Section 3.2, we did not use OMI TCNO<sub>2</sub> after 2015. The data has been processed using the methodology of Pope et al., (2018) to map the TCNO<sub>2</sub> data onto a high-resolution spatial grid (0.025° × 0.025°, ~2-3 km × ~2-3 km for TROPOMI, 0.05° × 0.05°, ~5 km × ~5 km for OMI). The TROPOMI data were quality controlled for a cloud radiance fraction <0.5, a quality control flag >0.75 and where the TCNO<sub>2</sub> value was > -1.0×10<sup>-5</sup> moles/m<sup>2</sup> (i.e. random values round 0.0 may be slightly negative or positive so we filter for TCNO<sub>2</sub> > -1.0×10<sup>-5</sup> moles/m<sup>2</sup> otherwise a positive bias in average TCNO<sub>2</sub> is imposed). While TROPOMI provides the greatest spatial resolution of any satellite instrument to measure air pollutants, suitable to derive TCNO<sub>2</sub> emission estimates over UK city-scale sources, the retrieved TCNO<sub>2</sub> has been shown to have a low bias. Over north-western Europe, Verhoelst et al., (2021) found that TROPOMI underestimated TCNO<sub>2</sub> by approximately 20-30% when compared with surface TCNO<sub>2</sub> measurements, which is consistent with Chan et al., (2020) and Dimitropoulou et al., (2020). OMI data were processed for a geometric cloud fraction of <0.2, quality flag = 0 (which also flags pixels influenced by the row anomaly (Braak, 2010)) and TCNO<sub>2</sub> > -1.0×10<sup>-5</sup> moles/m<sup>2</sup>.

### 2.3 Simplified Mass Balance Approach

To derive top-down emissions of NO<sub>2</sub> we use the SMBA, which is based on downwind plumes of TROPOMI observed TCNO<sub>2</sub> from the target source where the observed total mass of NO<sub>2</sub> (i.e. the source-related enhancement of TCNO<sub>2</sub> above the background level) is assumed to be a product of the emission rate and the effective lifetime. Therefore, we can derive the emission rate based on **Equation 1**:

$$E = \frac{\sum_{i=0}^N (NO_2 LD_i \times \Delta d)}{t \times e^{\frac{-t}{\tau}}} \quad (1)$$

where  $E$  is the emission rate (moles/s),  $NO_2 LD$  is the NO<sub>2</sub> line density (moles/m),  $\Delta d$  is the grid box length (m),  $i$  is the grid box number between the source and background value,  $t$  is time (s) and  $e^{\frac{-t}{\tau}}$  is the e-folding loss term with  $\tau$  as the effective lifetime.  $N$  represents the number of satellite TCNO<sub>2</sub> grid boxes between the source and background level  $B$ .  $t$  is calculated as the distance between the source and  $B$  divided by the wind speed ( $ws$ ). To derive the full NO<sub>2</sub> loading emitted from the source, the wind flow  $NO_2 LD$  has the background  $NO_2 LD$  value subtracted from all points between the source and  $B$  and is then summed yielding the total NO<sub>2</sub> mass (moles).

The wind speed and direction at a particular source are determined from the European Centre for Medium-Range Weather Forecasts (ECMWF, 2021) ERA5 u- & v-wind component data. The wind data are sampled at 13:00 UTC (around 13:00 local time (LT) over the UK) to coincide with the TROPOMI overpass (i.e. 13:30 LT) and averaged across boundary layer pressure levels (i.e. surface to 900 hPa). In all cases, the  $ws$  had to be greater than 2 m/s to avoid near stable meteorological conditions. Studies such as Beirle et al. (2011) and Verstraeten et al. (2018) averaged the wind speeds over the surface to 500 m layer. Beirle et al. (2011) suggested that the average winds across this altitude range yielded uncertainties over approximately 30%, but neither study provided definitive reasoning why 500 m was selected. In the UK, 500 m is

approximately 950 hPa which sits comfortably within the boundary layer (approximately 1000 m or 880.0 to 910 hPa in **Figure 1a** based on ERA-5 data sampled at 13.00 LT and averaged for 2019). In this study, we argue that wind speeds throughout the boundary layer are likely to be important in controlling the spatial distribution of NO<sub>2</sub> downwind of sources. **Figure 1b** shows the zonally averaged latitude-pressure NO<sub>2</sub> profile from the Copernicus Atmosphere Monitoring Service (CAMS, 2021), sampled at 13.00 LT and averaged for 2019, over the UK. The bulk of the NO<sub>2</sub> loading is near the surface with NO<sub>2</sub> concentrations of 0.5 ppbv to >1.0 ppbv between the surface and 900 hPa. As shown by the white dashed lines, 60-70% of the surface to 500 hPa NO<sub>2</sub> loading exists between the surface and 900 hPa. The zonally averaged boundary layer pressure (red dashed line) also straddles the 900 hPa level. In **Figure 1c**, the wind speed profile for London sampled under westerly flow increases with altitude until between 925 hPa and 900 hPa. For each pressure level, London westerly days are defined based average u- and v-components between the surface and the respective pressure level. As shown by the blue text, the wind speed gradient with respect to pressure substantially decreases (i.e. from -0.0406 m/s/hPa between 950 hPa and 925 hPa to -0.0045 m/s/hPa between 925 hPa and 900 hPa) at 900 hPa. Therefore, this profile gradient and the information in **Figures 1a & b** suggest that 900 hPa is a suitable level to derive the boundary layer average wind speed and flow direction. The table (**panel d**) in **Figure 1** shows the sensitivity of the NO<sub>x</sub> emission parameters to the pressure layer used. The derivation of emissions is discussed further in this section. The surface-850 hPa average and surface only winds show substantially different NO<sub>x</sub> emission rates of 61.6 moles/s and 30.1 moles/s, respectively. However, the intermediate levels (900 hPa and 950 hPa) show less dramatic step changes with emission rates of 55.2 moles/s and 49.8 moles/s. Therefore, the surface-900 hPa layer is used to help derive NO<sub>x</sub> emission rates in this study.

The NO<sub>2</sub> LD is the product of the source width, which is perpendicular to the wind flow, and the source-width-average TCNO<sub>2</sub> profile downwind from the source on a grid box by grid box basis as shown in **Equation 2**.

$$NO_2LD_{i=1,N} = \frac{\sum_{j=1}^n TCNO_{2i,j}}{n} \times w \quad (2)$$

where NO<sub>2</sub> LD (moles/m) is the NO<sub>2</sub> line density, *i* the grid box index downwind of the source starting at *i*=1 going to *i*=*N* at background point *B*, TCNO<sub>2</sub> is the tropospheric column NO<sub>2</sub> grid box value (moles/m<sup>2</sup>) at point *i* and *j* is the grid box index for the number of grid boxes *n*, perpendicular to the downwind profile, which fit across the width of the source at grid box *i* downwind and *w* is the source width (m) (i.e. source width perpendicular to the downwind profile) of the NO<sub>2</sub> source. Though the source width is a subjective choice between the source edge locations, the same source width value is used when deriving the TROPOMI NO<sub>x</sub> emissions and summing up the NAEI NO<sub>x</sub> emissions over the source region. As the source emissions will be a function of the source width (i.e. larger at source centre and lower at source edge), the mean TCNO<sub>2</sub> downwind profile is representative of the source-average NO<sub>2</sub> emission.

**Figure 2a** shows the difference between TROPOMI TCNO<sub>2</sub> sampled under westerly flow and the long-term average based on London u- and v-wind components, where there are clear downwind positive anomalies >3.0×10<sup>-5</sup> moles/m<sup>2</sup>. Similarly in **Figure 2b**, the downwind plume (e.g. westerly flow over London) has typically larger NO<sub>2</sub> LD values than the all-flow (i.e. all wind directions) NO<sub>2</sub> LD. The full NO<sub>2</sub> mass emitted from the source in the NO<sub>2</sub> LD is

the summation of the wind-flow  $NO_2$  LD from source up to point  $B$  minus the background value from all downwind pixels over this profile segment. A reasonable estimate of when the wind-flow  $NO_2$  LD reaches  $B$ , for more isolated  $NO_2$  sources, is when it intersects with the all-flow  $NO_2$  LD profile (i.e. returns to normal levels). However, when there are substantial upwind  $NO_2$  sources, this can yield wind-flow  $NO_2$  LD profiles which never intersect with the all-flow  $NO_2$  LD profile within the domain (e.g. see Birmingham example in **Figure 3a & b**). Therefore, to determine when  $B$  has been reached, a running t-test was applied to the wind-flow  $NO_2$  LD profile to determine where turning points or levelling off occurred. As such a test can be sensitive to noise in the TCNO<sub>2</sub> data, a 10-pixel (0.5°) running average wind-flow  $NO_2$  LD profile was calculated. The running t-test was applied to this using two windows of the same size to identify step changes in the profile. The green line in **Figure 2b** shows where the t-test p-value has become large and there is a turning point in the wind-flow  $NO_2$  LD profile. Such a reduction in the wind-flow  $NO_2$  LD profile gradient is suggestive of the plume reaching  $B$  as  $NO_2$  levels have stabilised. However, in **Figure 2b**, there are multiple locations potentially meeting this criteria. In reality, the turning points further downwind of London are sources from the Benelux region. The red dot represents the first instance, after the initial near-source wind-flow  $NO_2$  LD peak, where the gradient in the running t-test p-value profile changes sign (i.e. positive to negative or vice versa).

The loss term  $e^{-\frac{t}{\tau}}$  is dependent upon  $\tau$  and is determined by applying an e-folding distance fit between the near-source peak wind-flow  $NO_2$  LD value and  $B$ , before dividing by  $ws$  to get  $\tau$ . Here, a range of e-folding distances are tested in the loss term  $e^{-\frac{t}{\tau}}$  to find the distance value which yields the lowest root mean square error (RMSE), and a large  $R^2$  (Pearson correlation coefficient squared) value, between the e-folding distance fit (red line, **Figure 2c**) and the wind-flow  $NO_2$  LD (black line, **Figure 2c**). In the case of London, this yielded an e-folding distance of 148.0 km and  $\tau$  of 4.5 hours (8.6 and 3.1 hours) based on the average  $ws = 9.1$  m/s with an uncertainty range ( $\pm 4.3$  m/s; i.e.  $\pm 1$ -sigma standard deviation) of 4.8 m/s to 13.4 m/s (i.e. a slower/faster wind speed yields a longer/shorter lifetime). The effective lifetime derived here for London and other UK cities is typically consistent with values from other studies (e.g. Beirle et al., (2011) and Verstraeten et al. (2018)) for European cities (i.e. 1.0 – 10.0 hours).

The top-down  $E$  is calculated from **Equation 1**, but this is an emissions flux of  $NO_2$  moles/s which needs to be converted to  $NO_x$  for comparison with the bottom-up inventories. This is done by scaling the  $NO_2$  emissions by 1.32 based on the  $NO:NO_2$  concentration ratio (0.32) in urban environments at midday (Seinfeld and Pandis, 2006; Liu et al., 2016). Verstraeten et al., (2018) used modelled  $NO$  and  $NO_2$  concentrations to derive a scaling more representative of the chemistry of the source. They estimate there is a 10% uncertainty (similar to Beirle et al., (2011)), but as the modelled  $NO_2:NO_x$  ratio is based on the input emissions, for which the satellite data is being used to evaluate, this process is rather circular and not independent. The final emission uncertainty estimates (**Figure 2**) are derived by  $\pm$  the satellite error ( $10^{-5}$  moles/m<sup>2</sup>) before obtaining the  $NO_2$  LD (Sat  $NO_x$  Emissions-1) and by using the uncertainties in  $\tau$  when determining the loss term (Sat  $NO_x$  Emissions-2).

Here, the top-down  $NO_x$  emissions are derived by sampling TCNO<sub>2</sub> data under different wind directions in all seasons. Several studies, such as Beirle et al. (2011), have gone a step further and used TCNO<sub>2</sub> data to derive seasonal emissions. Unfortunately, here we are restricted to

looking at annually derived emissions due to 1) the TROPOMI TCNO<sub>2</sub> record only started in February 2018, 2) the COVID-19 pandemic resulted in a dramatic reduction in UK (and global) NO<sub>x</sub> emissions (Potts et al., 2021) meaning TCNO<sub>2</sub> data beyond February 2020 could not be used to derive top-down emissions under normal conditions and 3) the UK is subject to frequently cloudy conditions yielding a reduction in the number of observations from TROPOMI. The latter point predominantly influences TROPOMI retrievals in the winter-time. Therefore, even though we sample TCNO<sub>2</sub> data in all seasons, there is likely to be a tendency towards summer-time TCNO<sub>2</sub> values, when TCNO<sub>2</sub> values tend to be lower (e.g. Pope et al., 2015), potentially leading to a low bias in the derived top-down NO<sub>x</sub> emissions.

### 3. Results

#### 3.1 NO<sub>x</sub> Sources

Surface emissions and observed TCNO<sub>2</sub> represent different quantities and are influenced by different processes. However, the short NO<sub>2</sub> lifetime of a few hours (Schaub et al., 2007; Pope et al., 2015) means there is a sharp gradient between sources and the background levels. Therefore, we can use the satellite TCNO<sub>2</sub> observations to provide some constraint on the spatial distribution of the NO<sub>x</sub> emissions. In **Figure 4**, spatial maps over south-eastern (**Figure 4a & c**) and northern England (**Figure 4b & d**) show evidence of co-located TCNO<sub>2</sub> and NO<sub>x</sub> emission hot spots, especially over many of the UK cities shown by circles. Here, both data sets have been mapped onto the spatial resolution of 0.025° × 0.025°. In South East England, TCNO<sub>2</sub> and NO<sub>x</sub> emissions peak over London at over 14.0×10<sup>-5</sup> moles/m<sup>2</sup> and approximately >2.0 µg/m<sup>2</sup>/s, respectively. A secondary peak is also observed over western London for both quantities at similar levels. There are further co-located hotspots over Southampton (TCNO<sub>2</sub> ~8.0-9.0×10<sup>-5</sup> moles/m<sup>2</sup>, NO<sub>x</sub> >2.0 µg/m<sup>2</sup>/s), Portsmouth (TCNO<sub>2</sub> ~6.0-7.0×10<sup>-5</sup> moles/m<sup>2</sup>, NO<sub>x</sub> ~1.0-1.5 µg/m<sup>2</sup>/s), Brighton (TCNO<sub>2</sub> ~5.0-6.0×10<sup>-5</sup> moles/m<sup>2</sup>, NO<sub>x</sub> ~0.5-0.8 µg/m<sup>2</sup>/s), Oxford (TCNO<sub>2</sub> ~7.0-7.5×10<sup>-5</sup> moles/m<sup>2</sup>, NO<sub>x</sub> ~0.7-1.0 µg/m<sup>2</sup>/s) and Chelmsford (TCNO<sub>2</sub> ~8.5-9.5×10<sup>-5</sup> moles/m<sup>2</sup>, NO<sub>x</sub> ~0.5 µg/m<sup>2</sup>/s). In northern England and the Midlands, peak TCNO<sub>2</sub> and NO<sub>x</sub> emissions are located over Manchester (TCNO<sub>2</sub> ~10.0-11.0×10<sup>-5</sup> moles/m<sup>2</sup>, NO<sub>x</sub> ~1.0-1.5 µg/m<sup>2</sup>/s), Birmingham (TCNO<sub>2</sub> ~8.0-9.0×10<sup>-5</sup> moles/m<sup>2</sup>, NO<sub>x</sub> ~1.0-1.5 µg/m<sup>2</sup>/s), Leeds (TCNO<sub>2</sub> ~8.0-9.0×10<sup>-5</sup> moles/m<sup>2</sup>, NO<sub>x</sub> ~1.0-1.5 µg/m<sup>2</sup>/s) and Liverpool (TCNO<sub>2</sub> ~7.0-8.0×10<sup>-5</sup> moles/m<sup>2</sup>, NO<sub>x</sub> ~0.5-1.0 µg/m<sup>2</sup>/s).

To quantify the spatial relationship between the TCNO<sub>2</sub> and NO<sub>x</sub> emissions over source regions, the corresponding pixels of both data sets were sub-sampled for each UK city (79 in total), normalised by the sample mean and correlated against each other (red circles, **Figure 4e**), which yielded a correlation  $R_{\text{city}1\times1} = 0.35$  (i.e. city1×1 represents 1 grid box × 1 grid box or 0.025° × 0.025° around where the city centre is located). However, as atmospheric NO<sub>2</sub> is subject to chemical reactions and meteorological processes (e.g. transport), the signal around source regions is more diluted and the peak TCNO<sub>2</sub> not necessarily centred on the source. To allow for that, the spatial resolution of the quantities over each source was degraded, averaging over 3×3 (**Figure 4f**), 5×5 (**Figure 4g**) and 7×7 (**Figure 4h**) grid cells and the correlation recalculated (e.g. city3×3 represents 3 grid boxes × 3 grid boxes or 0.075° × 0.075° around where the city centre is located). This resulted in correlations of  $R_{\text{city}3\times3} = 0.53$ ,  $R_{\text{city}5\times5} = 0.62$  and  $R_{\text{city}7\times7} = 0.52$ . The correlation for full domain (i.e. the UK) was  $R_{\text{all}} = 0.20$ . As expected, the correlation for all grid pixels (e.g. including pixels over the sea) is weak where

long-range transport of NO<sub>2</sub> can yield spatial variability in background regions with corresponding zero emission pixels. The  $R_{city1 \times 1}$ ,  $R_{city3 \times 3}$ ,  $R_{city5 \times 5}$  and  $R_{city7 \times 7}$  correlations were all larger. The largest city-scale correlation was for the  $R_{city5 \times 5}$  values where the spatial variability has been smoothed and is representative of the more diffuse pattern of TCNO<sub>2</sub>. However, the  $R_{city7 \times 7}$  ( $0.175^\circ \times 0.175^\circ$  or  $\sim 15\text{-}20\text{ km} \times 15\text{-}20\text{ km}$ ) correlation is lower than the  $R_{city5 \times 5}$  value suggesting that this scale is larger than most UK city sizes. Overall, for all R values, except for  $R_{all}$ , there are statistically significant positive correlations at the 90% confidence level (CL) or above ( $>95\%$  CL for  $R_{city3 \times 3}$ ,  $R_{city5 \times 5}$  and  $R_{city7 \times 7}$ ). Therefore, the city-scale emission-satellite correlations provide confidence in the spatial distribution of the NAEI NO<sub>x</sub> emissions based on the observed satellite TCNO<sub>2</sub>.

### 3.2 Satellite NO<sub>2</sub> and Emission NO<sub>x</sub> Trends

To evaluate the temporal evolution of the NAEI emissions, we use the long-term satellite record of TCNO<sub>2</sub> from OMI between 2005 and 2015. Annual total UK emissions of NO<sub>x</sub> (expressed as NO<sub>2</sub> here) from the NAEI start in 1970 and continue to present day (typically with a lag of approximately two years). Annual spatial maps of the NAEI also exist over the same time period. However, while there is a consistent methodology for the UK total estimates, the mapping methodology updates between years (NAEI, 2017). Therefore, instead of performing trends on the maps, we focus on trends in the UK NO<sub>x</sub> emission totals. For OMI, we have taken a similar broad scale approach focussing on averaged TCNO<sub>2</sub> across England (defined as  $3^\circ\text{W}\text{-}2^\circ\text{E}$ ,  $50\text{-}54^\circ\text{N}$ ). We focus on England as the majority of large UK sources with reasonable spatiotemporal coverage are located here and have clearly defined trends over source regions. Pope et al., (2018) showed significantly (at the 95% CL) decreasing trends over London, Birmingham, Manchester and the Yorkshire power stations of between 1.5% and 2.3% per year. OMI measurements can be subject to large uncertainties and variability, so this analysis also investigates trends in a range of OMI TCNO<sub>2</sub> percentiles over time. To estimate the annual absolute England total NAEI NO<sub>x</sub> emissions, we summed the emissions data for England (same geographical definition as for OMI above) from the 2019 NAEI NO<sub>x</sub> emissions map and imposed the UK total NO<sub>x</sub> trend on it. Here, we use a simple linear fit which yields an annual decrease in the UK total NO<sub>x</sub> emission of 4.4%. The relative rate of change is the same for the England total NO<sub>x</sub> emissions, but the absolute values are lower than the UK total NO<sub>x</sub> emissions (**Figure 5, top panel**).

Over the 2005-2015 period, the England average OMI TCNO<sub>2</sub> trends in the 10<sup>th</sup>, 25<sup>th</sup>, 50<sup>th</sup>, 75<sup>th</sup> and 90<sup>th</sup> percentiles are  $-0.18 \times 10^{-5}$  moles/m<sup>2</sup>/yr (-3.3%/yr),  $-0.20 \times 10^{-5}$  moles/m<sup>2</sup>/yr (-2.7%/yr),  $-0.21 \times 10^{-5}$  moles/m<sup>2</sup>/yr (-2.2%/yr),  $-0.17 \times 10^{-5}$  moles/m<sup>2</sup>/yr (-1.3%/yr) and  $-0.07 \times 10^{-5}$  moles/m<sup>2</sup>/yr (-0.4%/yr), respectively (**Figure 5**). All of the satellite trends are significant at the 95% CL except for the 90<sup>th</sup> percentile. The UK and England total NO<sub>x</sub> emission trends between 2005 and 2015 are -76.3 kt/yr and -45.5 kt/yr (both -4.4%/yr). The OMI TCNO<sub>2</sub> trends range between -3.2% and -0.4% depending on the data percentile used to generate the average England TCNO<sub>2</sub> annual time series. We also calculated annual trends in UK and England (same definition as above) surface NO<sub>2</sub> observations (**Figure 5, bottom panel**) from AURN (AURN, 2021). Here, we used urban background, suburban and rural sites. For the 10<sup>th</sup>, 25<sup>th</sup>, 50<sup>th</sup>, 75<sup>th</sup> and 90<sup>th</sup> percentiles, UK (England) trends are -0.26 (-0.27) µg/m<sup>3</sup>/yr, -0.40 (-0.52) µg/m<sup>3</sup>/yr, -0.73 (-0.77) µg/m<sup>3</sup>/yr, -0.95 (-0.95) µg/m<sup>3</sup>/yr and -1.19 (-1.09) µg/m<sup>3</sup>/yr. This corresponds to -3.77 (-3.03) %/yr, -3.07 (-3.24) %/yr, -3.03 (-2.86) %/yr, -2.49 (-2.31) %/yr and



-2.29 (-1.98) %/yr. Therefore, the NAEI NO<sub>x</sub> emissions trend is of similar magnitude and direction to that of the observations. The differences are most likely explained by the non-linear conversion of emissions to atmospheric concentrations (i.e. complex meteorology and chemistry). The likely drivers for decreases in UK NO<sub>x</sub> emissions and NO<sub>2</sub> concentrations include a shift to cleaner energy sources (e.g. National Emissions Ceilings Regulations 2018, DEFRA. (2018b)), regulations on industrial and power generation emissions (Environmental Permitting Regulations 2016 (UK Government, 2016)) and tighter emissions for vehicles (e.g. Euro 6 emissions standards). Overall, these results provide confidence in the use of the satellite data as a tool to evaluate bottom-up emission trends.

### 3.3 Top-Down NO<sub>x</sub> Emissions

The top-down NO<sub>x</sub> emission rate for London under westerly flow (**Figure 2**) is 55.2 moles/s (35.5, 74.8 moles/s, based on Sat NO<sub>x</sub> Emissions-1 uncertainties), while the NAEI flux is 30.9 moles/s. Here, the NAEI has a low bias with the top-down estimate and sits outside the uncertainty range (though just sits within the Sat NO<sub>x</sub> Emissions-2 uncertainties). The top-down emissions are based on 2 years, so the flux should be representative of an annual emission rate, corresponding to the NAEI reporting. In the case of Birmingham (**Figure 3a**), under easterly flow, there is a visible plume (i.e. positive differences of  $2.0\text{--}3.0 \times 10^{-5}$  moles/m<sup>2</sup>) superimposed on a background enhancement ( $0.5\text{--}1.0 \times 10^{-5}$  moles/m<sup>2</sup>). As a result, the wind-flow NO<sub>2</sub> LD is always larger than the all-flow NO<sub>2</sub> LD and never reaches the background level (i.e. zero differences in **Figure 3a**) within the domain for which the TROPOMI TCNO<sub>2</sub> data has been processed for (e.g. there are positive differences in between the source, Birmingham, and the west of the domain, 8°W). Therefore, the running t-test methodology is used to determine when the wind-flow NO<sub>2</sub> LD reaches a steady background state *B*, as shown in **Figure 3b**. Overall, the NAEI (12.9 moles/s) underestimates the top-down emissions for Birmingham under easterly flow (29.0 (18.7, 39.2) moles/s).

Our methodology was applied to 10 city sources where sources had suitable downwind TCNO<sub>2</sub> enhancements to derive NO<sub>2</sub> LDs and top-down emissions (**Figure 6**). A suitable downwind TCNO<sub>2</sub> enhancement was subjectively identified when a clear TCNO<sub>2</sub> enhancement (i.e. positive anomalies) under a specific wind flow/direction occurred and a realistic lifetime (i.e. in the range of the literature – e.g. Verstraeten et al. (2018)) could be derived from the downwind TCNO<sub>2</sub> profile of the target source. These are shown in **Table 1**. Where top-down emissions could be derived for sources over several wind directions, they were averaged together. The TCNO<sub>2</sub> response to mesoscale and synoptic weather systems (i.e. large scale flow) can be seasonally influenced (e.g. Pope et al., 2015) with some wind directions occurring more frequently in certain seasons. Therefore, top-down NO<sub>x</sub> emission estimates derived from several wind directions for a particular source, though sampled throughout all months, can vary depending on the seasonal influence on the observed TCNO<sub>2</sub> for which the wind direction more frequently occurs in. The top-down emissions derived here suggest that the NAEI bottom-up emissions for the largest sources such as London, Manchester and Birmingham are underestimated. The top-down emissions for London, Manchester and Birmingham are 47.9 (31.7, 64.0) moles/s, 20.5 (13.0, 28.1) moles/s and 22.1, (14.5, 29.8) moles/s with corresponding NAEI emissions of 30.9 moles, 10.0 moles/s and 12.9 moles/s, respectively.

For the smaller sources (e.g. Edinburgh, Bristol and Cardiff), the comparisons are in better agreement with the NAEI and are located within the top-down emission ranges. However, for Newcastle the NAEI emissions (3.1 moles/s) are substantially larger than the top-down estimate (1.7 (0.8, 2.6) moles/s). In contrast, for Leeds (3.4 moles/s), Norwich (1.0 moles/s and Belfast (1.6 moles), the NAEI substantially underestimates the top-down emissions of 5.70 (3.7, 7.6) moles/s, 2.4 (1.3, 3.4) moles/s and 3.4 (2.1, 4.8) moles/s, respectively. For the NO<sub>2</sub> effective lifetime, we find it ranges between 2.9 and 7.9 hours, which is consistent with values in the literature (e.g. Schaub et al., 2007; Pope et al., 2015). For all cities in **Figure 6** there is a strong correlation (0.99) between the NAEI and top-down emission sources investigated here, but the NAEI has a low bias of -4.18 moles/s (-37.4%) on average, dominated by the larger sources (i.e. London, Manchester and Birmingham). These metrics were calculated in linear space.

#### 4. Conclusions

We have evaluated relationships between satellite observations (TROPOspheric Monitoring Instrument, TROPOMI) of tropospheric column nitrogen dioxide (TCNO<sub>2</sub>) and the UK National Atmospheric Emissions Inventory (NAEI) for nitrogen oxides (NO<sub>x</sub> = NO + NO<sub>2</sub>). Although they are different quantities, the short NO<sub>2</sub> lifetime means that our comparison can serve as a useful and important tool to evaluate bottom-up emissions. Here, spatial comparison of the TROPOMI TCNO<sub>2</sub> with the NAEI highlights consistency over the source regions with co-located peak values in the respective data sets. Correlation analysis of TCNO<sub>2</sub> and NO<sub>x</sub> emissions over the UK cities indicates moderate spatial agreement with R ranging between 0.4 and 0.6 (significant at the >90% confidence level). Analysis of long-term satellite records of TCNO<sub>2</sub> (from the Ozone Monitoring Instrument (OMI), 2005-2015) show comparable negative trends with the NAEI NO<sub>x</sub> emissions with rates of -2.2%/yr and -4.4%/yr, respectively. Though the relative NAEI trend is larger than OMI, meteorological conditions and photochemistry will control the atmospheric response to a change in NO<sub>x</sub> emissions, as seen by OMI. It is also possible that the NAEI overestimates the decreasing NO<sub>x</sub> emissions trend.

We have also used TROPOMI data to derive top-down city-scale estimates of UK NO<sub>x</sub> emissions. While it can still be challenging to derive emissions from city scale sources (e.g. frequent cloud cover in the UK), we estimate top-down emissions fluxes (using satellite data between February 2018 and January 2020) for several cities. Most of the city sources show reasonable agreement, but for larger sources like London, Manchester and Birmingham, the top-down emission values are substantially larger than those in the NAEI for 2019. Overall, as far as we are aware, this study represents the first robust attempt to use satellite observations of TCNO<sub>2</sub> to evaluate and constrain the official UK bottom-up NAEI. We find spatial and temporal agreement between the two quantities, but find evidence that the NAEI NO<sub>x</sub> emissions for larger sources (e.g. London) may be too low (i.e. by >25%) sitting outside the top-down emission uncertainty ranges (i.e. based on the satellite retrieval errors). To fully understand the discrepancies and the drivers of these NO<sub>x</sub> emissions differences, further investigation is required.

## Data Availability

TROPOMI and OMI tropospheric column NO<sub>2</sub> data comes from the Tropospheric Emissions Monitoring Internet Service (TEMIS, <https://www.temis.nl/airpollution/no2.php>). The bottom-up NO<sub>x</sub> emissions come from the National Atmospheric Emissions Inventory (<https://naei.beis.gov.uk/data/data-selector?view=air-pollutants>) and the point and area sources can be obtained from [https://naei.beis.gov.uk/data/map-uk-das?pollutant\\_id=6&emiss\\_maps\\_submit=naei-20210325121854](https://naei.beis.gov.uk/data/map-uk-das?pollutant_id=6&emiss_maps_submit=naei-20210325121854). The specific UK total NO<sub>x</sub> emissions came from <https://naei.beis.gov.uk/data/data-selector-results?q=142818>. Meteorological wind, temperature and boundary layer height data came from ECMWF (<https://cds.climate.copernicus.eu/cdsapp#!/dataset/reanalysis-era5-pressure-levels?tab=overview>). CAMS NO<sub>2</sub> data was retrieved from <https://ads.atmosphere.copernicus.eu/cdsapp#!/dataset/cams-global-reanalysis-eac4?tab=form>. The AURN data was obtained from <https://uk-air.defra.gov.uk/networks/network-info?view=aurn>.

## Author contribution

RJP undertook the research looking at the spatial maps and long-term trends. RJP, RK, CW and AMG worked on the satellite top-down city-scale NO<sub>x</sub> emission estimates. RJP prepared the manuscript with contributions from all co-authors.

## Competing interests

The authors declare that they have no conflict of interest.

## Acknowledgements

This work was funded by the Department for Environment, Food and Rural Affairs Affairs through the “Applying Earth Observation (EO) to Reduce Uncertainties in Emission Inventories” project and by the UK Natural Environment Research Council (NERC) by providing funding for the National Centre for Earth Observation (NCEO, award reference NE/R016518/1).

## References

- AURN. Automated Urban and Rural Network [Online]. Available: <https://uk-air.defra.gov.uk/networks/network-info?view=aurn> (accessed 30<sup>th</sup> March 2021), 2021.
- Beirle, S., Boersma, B.F., Platt, U., Lawrence, M.G. and Wagner, T.: Megacity emissions and lifetimes of nitrogen oxides probed from space, *Science*, 333, 1737, doi:10.1126/science.1207824, 2011.
- Boersma, K.F., Eskes, H.J., Veefkind, J.P., Brinksma, E.J., van der A, R.J., Sneep, M., van den Oord, G.H.J., Levelt, P.F., Stammes, P., Gleason, J.F. and Bucsela, E.J.: Near-real time retrieval of tropospheric NO<sub>2</sub> from OMI, *Atmospheric Chemistry and Physics*, 7, 2103–2118, doi:10.5194/acp-7-2103-2007, 2007.
- Braak R. 2010. Row Anomaly Flagging Rules Lookup Table, KNMI Technical Document TN-OMIE-KNMI-950, *KNMI*, Netherlands.
- CAMS. CAMS global reanalysis (EAC4). Available: <https://ads.atmosphere.copernicus.eu/cdsapp#!/dataset/cams-global-reanalysis-eac4?tab=form> (accessed 29<sup>th</sup> November 2021), 2021.

515

516 Chan, K. L., Wiegner, M., van Geffen, J., De Smedt, I., Alberti, C., Cheng, Z., Ye, S. and Wenig,  
517 M.: MAX-DOAS measurements of tropospheric NO<sub>2</sub> and HCHO in Munich and the  
518 comparison to OMI and TROPOMI satellite observations, *Atmospheric Measurement*  
519 *Techniques*, 13, 4499–4520, doi: 10.5194/amt-13-4499-2020, 2020.

520 DEFRA. Air Pollution in the UK 2017 [Online]. Available: [https://uk-](https://uk-air.defra.gov.uk/assets/documents/annualreport/air_pollution_uk_2017_issue_1.pdf)  
521 [air.defra.gov.uk/assets/documents/annualreport/air\\_pollution\\_uk\\_2017\\_issue\\_1.pdf](https://uk-air.defra.gov.uk/assets/documents/annualreport/air_pollution_uk_2017_issue_1.pdf) (last  
522 accessed 30<sup>th</sup> March 2021), 2018a.

523 DEFRA. UK Informative Inventory Report (1990 to 2016) [Online]. Available: [https://uk-](https://uk-air.defra.gov.uk/library/reports?report_id=956)  
524 [air.defra.gov.uk/library/reports?report\\_id=956](https://uk-air.defra.gov.uk/library/reports?report_id=956) (last accessed 30<sup>th</sup> March 2021), 2018b.

525 DEFRA. Air Pollution in the UK 2019 [Online]. Available: [https://uk-](https://uk-air.defra.gov.uk/library/annualreport/viewonline?year=2019_issue_1#report_pdf)  
526 [air.defra.gov.uk/library/annualreport/viewonline?year=2019\\_issue\\_1#report\\_pdf](https://uk-air.defra.gov.uk/library/annualreport/viewonline?year=2019_issue_1#report_pdf) (accessed  
527 30<sup>th</sup> March 2021), 2020.

528 Dibbens, C. and Clemens, T.: Place of work and residential exposure to ambient air pollution  
529 and birth outcomes in Scotland, using geographically fine pollution climate mapping  
530 estimates, *Environmental Research*, 140, 535–541, doi:10.1016/j.envres.2015.05.010,  
531 (2015).

532 Dimitropoulou, E., Hendrick, F., Pinardi, G., Friedrich, M. M., Merlaud, A., Tack, F., De  
533 Loungeville, H., Fayt, C., Hermans, C., Laffineur, Q., Fierens, F. and Van Roozendaal, M.:  
534 Validation of TROPOMI tropospheric NO<sub>2</sub> columns using dual-scan multi-axis differential  
535 optical absorption spectroscopy (MAX-DOAS) measurements in Uccle, Brussels, *Atmospheric*  
536 *Measurement Techniques*, 13, 5165–5191, doi: 10.5194/amt-13-5165-2020, 2020.

537 ECMWF. ERA5 hourly data on pressure levels from 1979 to present. Available at:  
538 [https://cds.climate.copernicus.eu/cdsapp#!/dataset/reanalysis-era5-pressure-](https://cds.climate.copernicus.eu/cdsapp#!/dataset/reanalysis-era5-pressure-levels?tab=overview)  
539 [levels?tab=overview](https://cds.climate.copernicus.eu/cdsapp#!/dataset/reanalysis-era5-pressure-levels?tab=overview) (accessed 29<sup>th</sup> November 2021), 2021.

540 EEA. Air quality in Europe — 2018 report [Online]. Available:  
541 <https://www.eea.europa.eu/publications/air-quality-in-europe-2018> (accessed 30<sup>th</sup> March  
542 2021), 2018.

543 EMEP/EEA. EMEP/EEA air pollutant emission inventory guidebook 2019, EEA Report No  
544 13/2019, ISSN 1977-8449. Available: [https://www.eea.europa.eu/publications/emep-eea-](https://www.eea.europa.eu/publications/emep-eea-guidebook-2019)  
545 [guidebook-2019](https://www.eea.europa.eu/publications/emep-eea-guidebook-2019) (accessed 2<sup>nd</sup> July 2021), 2019.

546

547 EMEP. EMEP – Convention on Long-range Transboundary Air Pollution. Available:  
548 <https://www.emep.int/> (accessed 12<sup>th</sup> July 2021), 2021.

549

550 Liu, F., Beirle, S., Zhang, Q., Dörner, S., He, K. and Wagner T.: NO<sub>x</sub> lifetimes and emissions of  
551 cities and power plants in polluted background estimated by satellite observations,  
552 *Atmospheric Chemistry and Physics*, 16, 5283–5298, doi:10.5194/acp-16-5283-2016, 2016.

553 Martin, R.V., Jacob, D.J., Chance, K., Kurosu, T.P., Palmer, P.I. and Evans, M.J.: Global  
554 inventory of nitrogen oxide emissions constrained by space-based observations of NO<sub>2</sub>  
555 columns, *Journal of Geophysical Research*, 108, 4537, doi:10.1029/2003JD003453, 2003.

556 Miyazaki, K., Eskes, H., Sudo, K., Boersma, K.F., Bowman, K. and Kanaya, Y.: Decadal changes  
 557 in global surface NO<sub>x</sub> emissions from multi-consistent satellite data assimilation,  
 558 *Atmospheric Chemistry and Physics*, 17, 807–837, doi:10.5194/acp-17-807-2017, 2016.

559 NAEI. UK Emission Mapping Methodology. – 2015 [Online]. Available: [https://uk-](https://uk-air.defra.gov.uk/assets/documents/reports/cat07/1710261436_Methodology_for_NAEI_2017.pdf)  
 560 [air.defra.gov.uk/assets/documents/reports/cat07/1710261436\\_Methodology\\_for\\_NAEI\\_20](https://uk-air.defra.gov.uk/assets/documents/reports/cat07/1710261436_Methodology_for_NAEI_2017.pdf)  
 561 [17.pdf](https://uk-air.defra.gov.uk/assets/documents/reports/cat07/1710261436_Methodology_for_NAEI_2017.pdf) (accessed 30<sup>th</sup> March 2021), 2017.

562 NAEI. UK-NAEI – National Atmospheric Emissions Inventory [Online]. Available:  
 563 <https://naei.beis.gov.uk/> (accessed 30<sup>th</sup> March 2021), 2021.

564 Pena-Angulo, D., Reig-Gracia, F., Dominguez-Castro, F., Revuelto, J., Aguilar, E., van der  
 565 Schrier, G. and Vicente-Serrano, S. M.: ECTACI: European Climatology and Trends Atlas of  
 566 Climate Indices (1979–2017), *Journal of Geophysical Research: Atmospheres*, 125,  
 567 e2020JD032798, doi: 10.1029/2020JD032798, 2020. Pope, R.J., Savage, N.H., Chipperfield,  
 568 M.P., Ordonez, C. and Neal, L.S.: The influence of synoptic weather regimes on UK air  
 569 quality: Regional model studies of tropospheric column NO<sub>2</sub>, *Atmospheric Chemistry and*  
 570 *Physics*, 15, 11201–11215, doi:10.5194/acp-15-11201-2015, 2015.

571 Pope, R.J., Arnold, S.R., Chipperfield, M.P., Latter, B.G., Siddans, R. and Kerridge, B.J.:  
 572 Widespread changes in UK air quality observed from space, *Atmospheric Science Letters*, 19,  
 573 e817, doi: 10.1002/asl.817, 2018.

574 Potts, D.A., Marais, E.A., Boesch, H., Pope, R.J., Lee, J., Drysdale, W., Chipperfield, M.P.,  
 575 Kerridge, B. and Siddans, R.: Diagnosing air quality changes in the UK during the COVID-19  
 576 lockdown using TROPOMI and GEOS-Chem, *Environmental Research Letters*, 16, 054031,  
 577 doi:10.1088/1748-9326/abde5d, 2021.

578 Ricardo Energy and Environment. UK Informative Inventory Report (1990 to 2019).  
 579 Available: [https://uk-](https://uk-air.defra.gov.uk/assets/documents/reports/cat09/2103151107_GB_IIR_2021_FINAL.pdf)  
 580 [air.defra.gov.uk/assets/documents/reports/cat09/2103151107\\_GB\\_IIR\\_2021\\_FINAL.pdf](https://uk-air.defra.gov.uk/assets/documents/reports/cat09/2103151107_GB_IIR_2021_FINAL.pdf)  
 581 (accessed 2<sup>nd</sup> July 2021), 2021.

582 Royal College of Physicians. Every breath we take: the lifelong impact of air pollution  
 583 [Online]. Available: [https://www.rcplondon.ac.uk/projects/outputs/every-breath-we-take-](https://www.rcplondon.ac.uk/projects/outputs/every-breath-we-take-lifelong-impact-air-pollution)  
 584 [lifelong-impact-air-pollution](https://www.rcplondon.ac.uk/projects/outputs/every-breath-we-take-lifelong-impact-air-pollution) (accessed 30<sup>th</sup> March 2021), 2016.

585 Savage, N.H., Agnew, P., Davis, L.S., Ordóñez, C., Thorpe, R., Johnson, C.E., O'Connor, F.M.  
 586 and Dalvi, M.: Air quality modelling using the Met Office Unified Model (AQUM OS24-26):  
 587 model description and initial evaluation, *Geoscientific Model Development*, 6, 353–372,  
 588 doi:10.5194/gmd-6-353-2013, 2013.

589 Schaub, D., Brunner, D., Boersma, K.F., Keller, J., Folini, D., Buchmann, B., Berresheim, H.  
 590 and Staehelin, J.: SCIAMACHY tropospheric NO<sub>2</sub> over Switzerland: estimates of NO<sub>x</sub> lifetime  
 591 and impacts of the complex alpine topography on the retrieval, *Atmospheric Chemistry and*  
 592 *Physics*, 7, 5971–5987, doi:10.5194/acp-7-5971-2007, 2007.

593 Seinfeld, J. and Pandis, S.: Atmospheric Chemistry and Physics: From Air Pollution to Climate  
 594 Change - Second Edition, John Wiley and Sons Inc, New Jersey, USA, 2006.

Torres, O., Bhartia, P. K., Jethva, H. and Ahn, C.: Impact of the ozone monitoring instrument row anomaly on the long-term record of aerosol products, *Atmospheric Measurement Techniques*, 11, 2701-2715, doi:10.5194/amt-11-2701-2018, 2018.

Tsagatakis, I., Richardson, J., Evangelides, C., Pizzolato, M., Pearson, B., Passant, N., Pommier, M. and Otto, A.: UK Spatial Emissions Methodology: A report of the National Atmospheric Emission Inventory 2019. Available at: [https://uk-air.defra.gov.uk/assets/documents/reports/cat09/2107291052\\_UK\\_Spatial\\_Emissions\\_Methodology\\_for\\_NAEI\\_2019\\_v1.pdf](https://uk-air.defra.gov.uk/assets/documents/reports/cat09/2107291052_UK_Spatial_Emissions_Methodology_for_NAEI_2019_v1.pdf) (accessed 29th November 2021), 2021.

UK Government. The Environmental Permitting (England and Wales) Regulations 2016. Available: <https://www.legislation.gov.uk/uksi/2016/1154/contents/made> (last accessed 2<sup>nd</sup> July 2021), 2016.

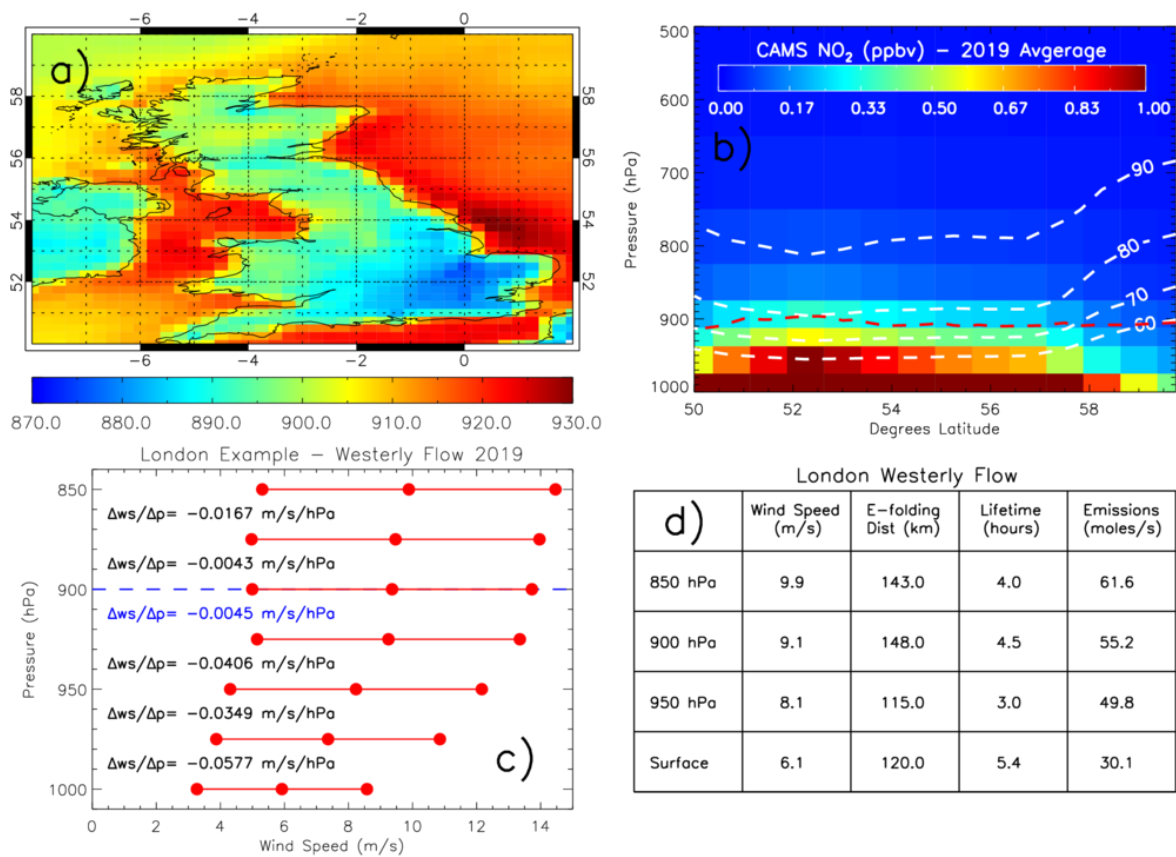
Veefkind, J.P., Aben, I., McMullan, K., Forster, H., de Vries, J., Otter, G., Claas, J., Eskes, H.J., de Haan, F., Kleipool, Q., van Weele, M., Hasekamp, O., Hoogeveen, R., Landgraf, J., Snel, R., Tol, P., Ingmann, P., Voors, R., Kruizinga, B., Vink, R., Visser, H. and Levelt, P.F.: TROPOMI on the ESA Sentinel-5 Precursor: A GMES mission for global observations of atmospheric composition for climate, air quality and ozone layer applications, *Remote Sensing of Environment*, 120, 70-83, doi:10.1016/j.rse.2011.09.027, 2012.

Verhoelst, T., Compernelle, S., Pinardi, G., Lambert, J. C., Eskes, H., Eichmann, K. U., et al.: Ground-based validation of the Copernicus Sentinel-5P TROPOMI NO<sub>2</sub> measurements with the NDACC ZSL-DOAS, MAX-DOAS and Pandonia global networks, *Atmospheric Measurement Techniques*, 14, 481–510, doi: 10.5194/amt-14-481-2021, 2021.

Verstraeten, W.W., Boersma, K.F., Douros, J., Williams, J.E., Eskes, H., Liu, F., Beirle, S. and Delcloo, A.: Top-down NO<sub>x</sub> emissions of European cities based on the downwind plume of modelled and space-borne tropospheric NO<sub>2</sub> column, *Sensors*, 18 (9), 2893, doi:10.3390/s18092893, 2018.

WHO. Ambient (outdoor) air pollution [Online]. Available: [https://www.who.int/news-room/fact-sheets/detail/ambient-\(outdoor\)-air-quality-and-health](https://www.who.int/news-room/fact-sheets/detail/ambient-(outdoor)-air-quality-and-health) (last accessed 30<sup>th</sup> March 2021), 2018.

Wu, H., Reis, S., Lin, C. and Heal, M.R.: Effect of monitoring network design on land use regression models for estimating residential NO<sub>2</sub> concentration, *Atmospheric Environment*, 149, 24-33, doi:10.1016/j.atmosenv.2016.11.014, 2017.



635 **Figure 1:** a) ERA-5 UK boundary layer pressure (hPa) sampled at 13.00 LT (to coincide with  
636 the TROPOMI overpass time) and averaged for 2019. b) CAMS reanalysis zonal (8.0°W-2.0°E)  
637 average latitude-pressure NO<sub>2</sub> (ppbv) cross-section over the UK between the surface and 500  
638 hPa. White dashed lines represent the percentage of the surface-500 hPa NO<sub>2</sub> loading  
639 between the surface and the respective pressure levels. The red dashed line represents the  
640 zonal average boundary layer pressure (hPa). c) Average (surface to pressure level) wind  
641 speed (m/s), ± the standard deviation, profile over London under westerly flow (determined  
642 from the ERA-5 u-wind and v-wind components at each pressure level).  $\Delta w_s/\Delta p$  is the wind  
643 speed gradient between pressure levels. The blue text indicates the first small step change in  
644 the gradient indicative of reduced flow turbulence and a suitable surface-altitude range to  
645 average the winds speeds over. d) The table shows the impact to the NO<sub>x</sub> emission  
646 parameters when using different altitudes over which to average the wind speeds.  
647  
648

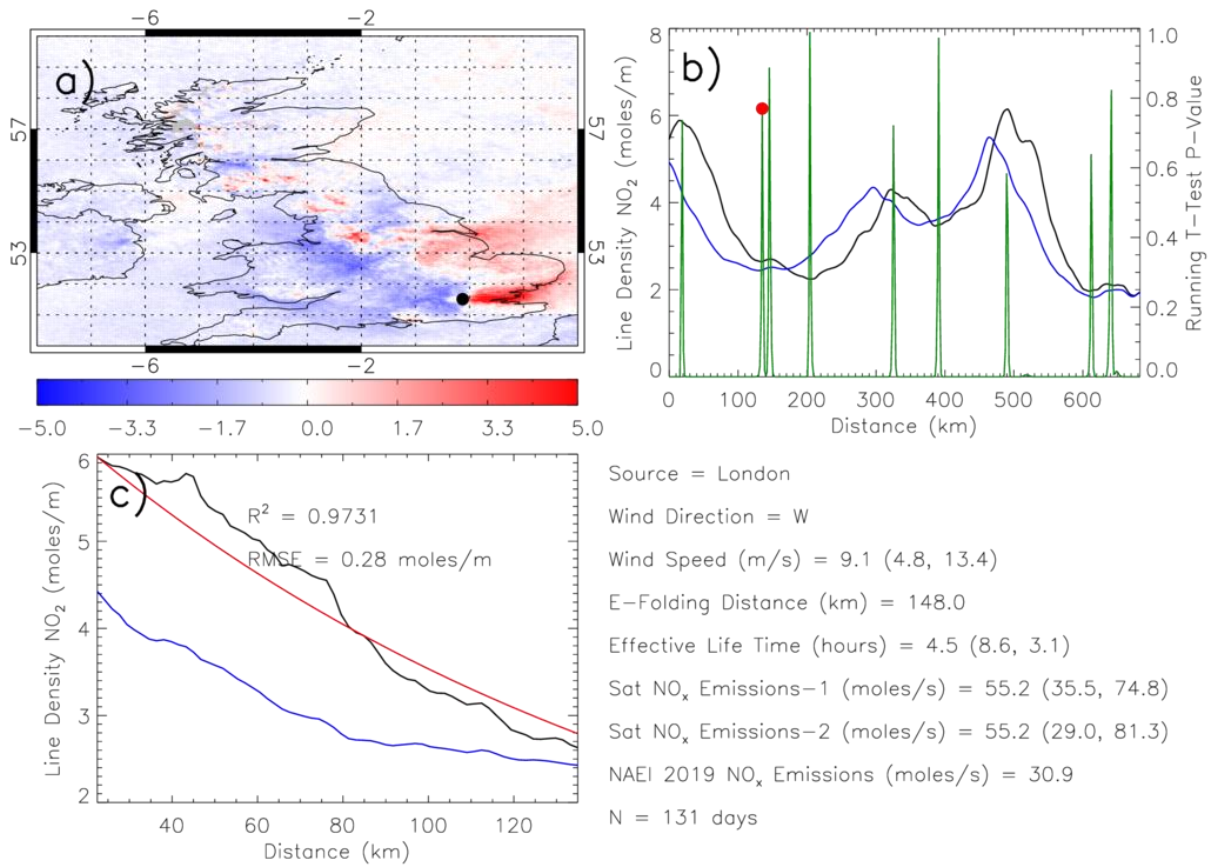


**Figure 2:** (a) TROPOMI TCNO<sub>2</sub> (10<sup>-5</sup> moles/m<sup>2</sup>) sub-sampled under westerly flow (defined over London, black dot) minus the long-term average (February 2018 to January 2020). (b) Downwind NO<sub>2</sub> LD from London (black = westerly flow, blue = all-flow average) with the corresponding running t-test p-value (green line). The red dot represents the location of background level determined by the turning point in the running t-test p-value time series. (c) The westerly flow and all-flow NO<sub>2</sub> LD between peak westerly flow NO<sub>2</sub> LD and the background value. The red line represents the e-folding distance fit with the corresponding  $R^2$  and root mean square error (RMSE) between the westerly flow NO<sub>2</sub> LD and fit profile.  $N$  represents the number of days classified under westerly flow over London.



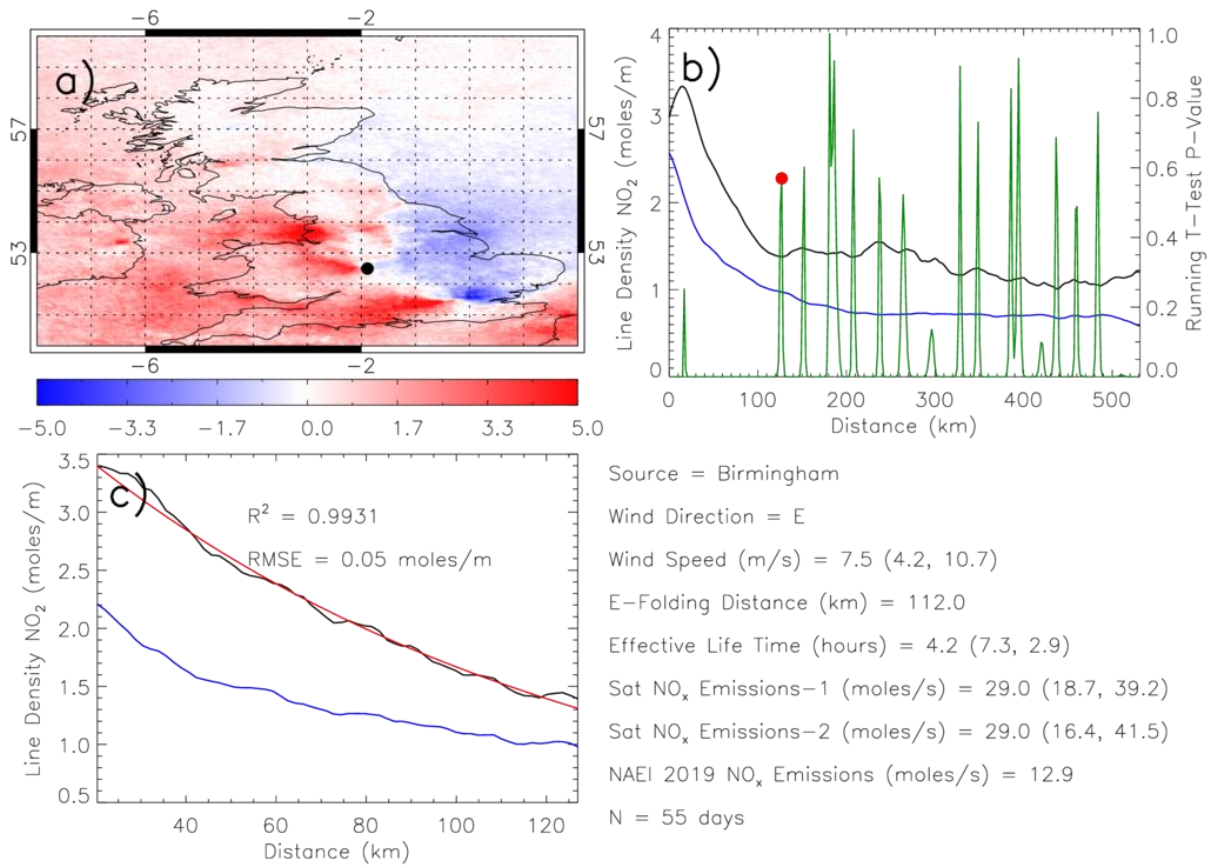
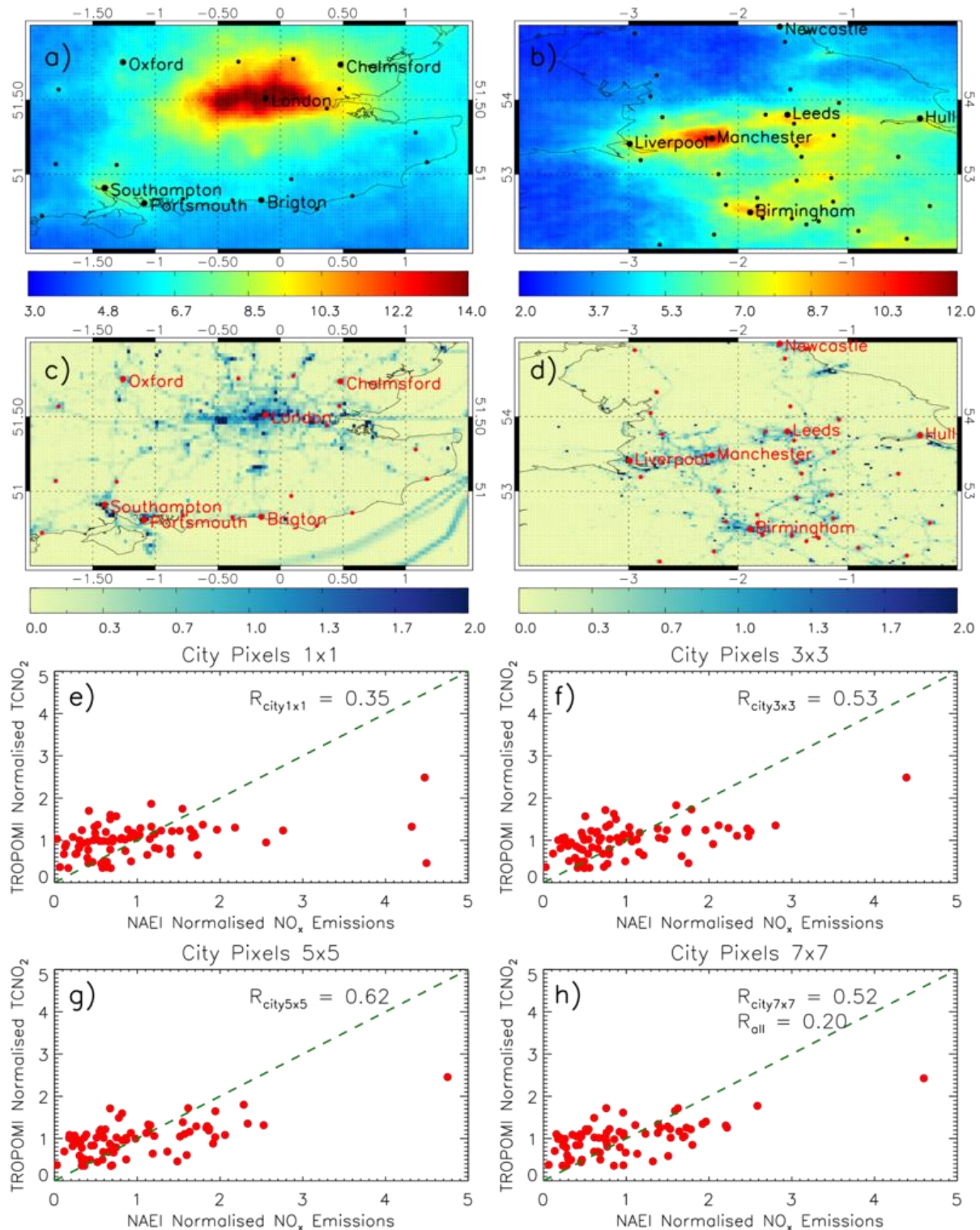


**Figure 3:** (a) TROPOMI TCNO<sub>2</sub> (10<sup>-5</sup> moles/m<sup>2</sup>) sub-sampled under easterly flow (defined over Birmingham, black dot) minus the long-term average (February 2018 to January 2020). (b) Downwind NO<sub>2</sub> LD from Birmingham (black = easterly flow, blue = all-flow average) with the corresponding running t-test p-value (green line). The red dot represents the location of background level determined by the turning point in the running t-test p-value time series. (c) The easterly flow and all-flow NO<sub>2</sub> LD between peak easterly flow NO<sub>2</sub> LD and the background value. The red line represents the e-folding distance fit with the corresponding  $R^2$  and root mean square error (RMSE) between the easterly flow NO<sub>2</sub> LD and fit profiles. N represents the number of days classified under easterly flow over Birmingham.



673

674

675 **Figure 4:** TROPOMI TCNO<sub>2</sub> ( $\times 10^{-5}$  moles/m<sup>2</sup>) average for February 2018 to January 2020

676 across (a) south-eastern and (b) northern England. Black circles represent city locations. NAEI

677 NO<sub>x</sub> emissions ( $\mu\text{g}/\text{m}^2/\text{s}$ ) for 2019 across (c) south-eastern and (d) northern England. Red678 circles represent city locations. Panels (e)-(h) represent the correlation of normalised TCNO<sub>2</sub>679 and NO<sub>x</sub> emissions for UK cities. The green dashed line is the 1:1 line. Each source is

normalised by the average of all the sources. The four panels also represent city means using

680    *varying pixel ranges around the source (i.e. 1×1, 3×3, 5×5 and 7×7 grid pixels). The*  
681    *correlations between the city-scale normalised NO<sub>x</sub> emissions and TCNO<sub>2</sub> are shown (R).*  
682

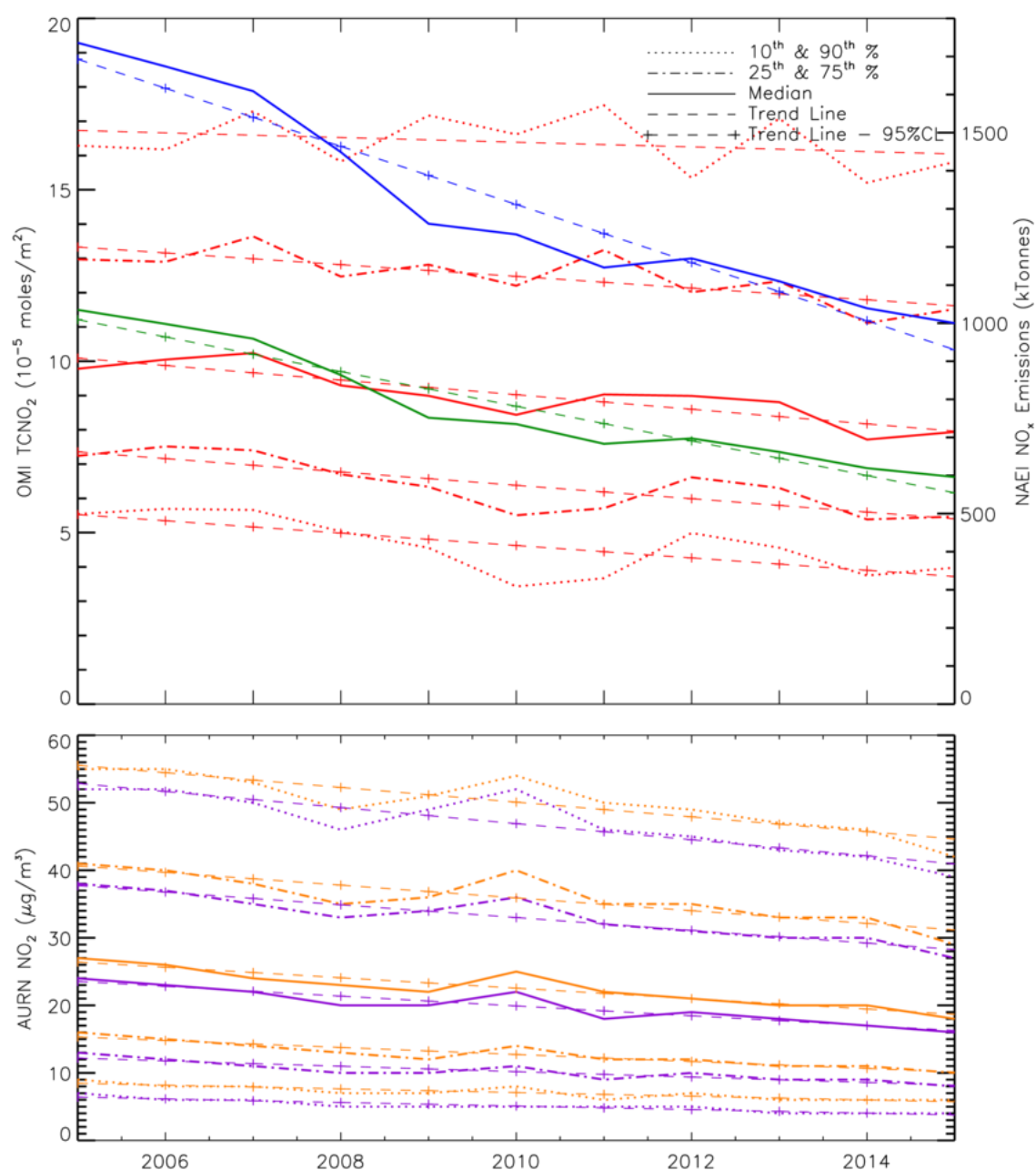


**Figure 5:** The top panel shows time series (2005 to 2015) in OMI TCNO<sub>2</sub> ( $\times 10^{-5}$  moles/m<sup>2</sup>) and NAEI NO<sub>x</sub> emission totals (kt or Gg). OMI median, 10<sup>th</sup> & 90<sup>th</sup> and 25<sup>th</sup> & 75<sup>th</sup> percentiles are represented by solid, dotted and dot-dashed lines, respectively. NAEI NO<sub>x</sub> emission totals for the UK and England are represented by the blue and green solid lines. Here, the OMI TCNO<sub>2</sub> has been averaged over England (defined as 3°W-2°E, 50-54°N) and while the UK NO<sub>x</sub> emission totals are directly reported by the NAEI, the England NO<sub>x</sub> emission totals have been summed over the emissions maps for the same England definition used for OMI (see Section 3.2 for more information). In the bottom panel, AURN surface NO<sub>2</sub> ( $\mu\text{g}/\text{m}^3$ ) times series are shown for the UK (purple) and England (orange). Trends lines are shown by dashed and dash-crossed lines for insignificant and significant trends (at the 95% confidence level).

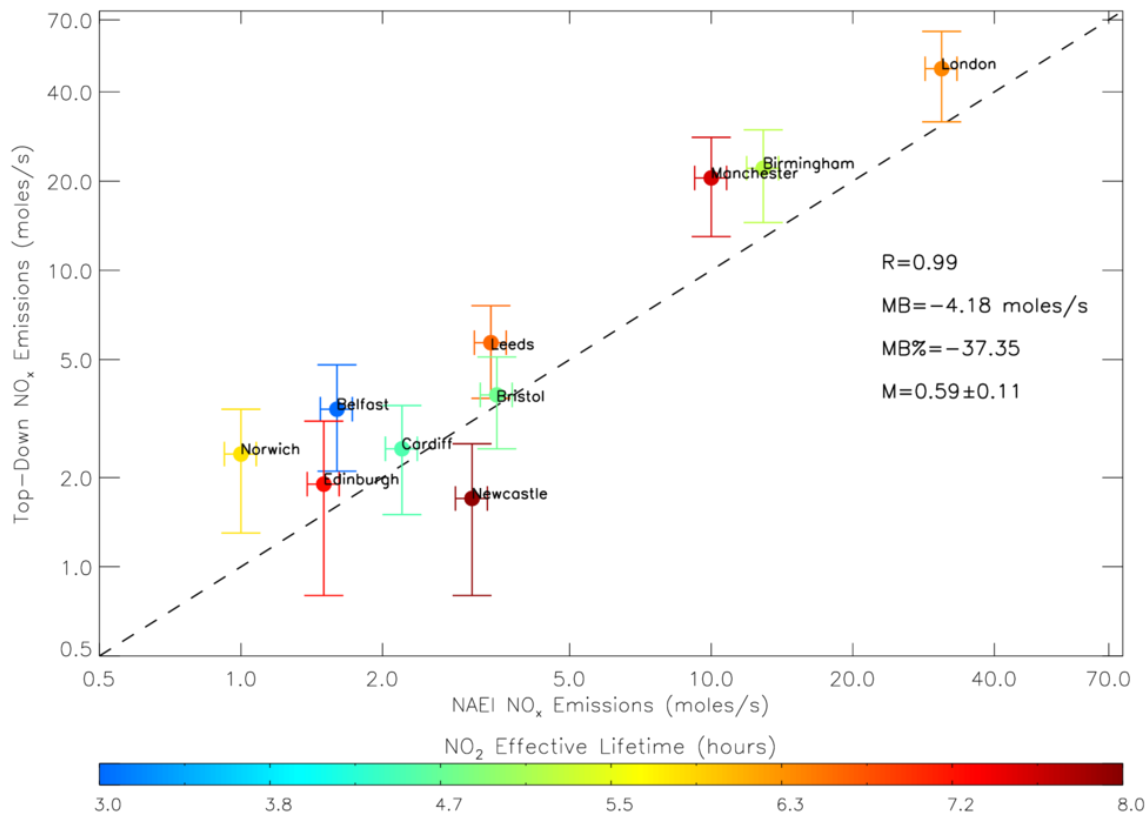


**Figure 6:** NAEI and top-down (TROPOMI)  $\text{NO}_x$  emissions (moles/s) for 10 UK cities coloured by the  $\text{NO}_2$  effective lifetime (hours). Where there is more than one top-down estimate for a city from multiple wind directions, the corresponding emission rates and lifetimes have been averaged together. The correlation ( $R$ ), mean bias ( $\text{MB}$ , moles/s), percentage mean bias ( $\text{MB\%}$ ) and linear fit ( $M$ ) are also shown. NAEI uncertainty is  $\pm 7.8\%$  (DEFRA, 2018b) and the top-down uncertainty range is based on satellite errors (i.e. Sat Emissions-1, see text). The black dashed line represents the 1:1 relationship and both axes are on log scales.

**Table 1:** List of top-down NO<sub>x</sub> (moles/s) emission estimates for UK city sources under different wind directions. Sat NO<sub>x</sub> Emissions-1 represents the emission flux estimated using the TROPOMI NO<sub>2</sub> ± the retrieval uncertainty, while Sat NO<sub>x</sub> Emissions-2 is based on the lifetime derived from the wind speed data ± 1.0 sigma standard deviation.

Source Name	London	London	London	Birmingham
Longitude	-0.13	-0.13	-0.13	-1.89
Latitude	51.51	51.51	51.51	52.50
Lon Edge - West	-0.52	-0.52	-0.52	-2.18
Lon Edge - East	0.28	0.28	0.28	-1.72
Lat Edge - South	51.32	51.32	51.32	52.35
Lat Edge - North	51.69	51.69	51.69	52.66
Wind Speed Average (m/s)	9.10	7.00	7.50	7.50
Wind Speed Standard Deviation (m/s)	4.30	3.20	3.10	3.20
Wind Direction	W	N	E	E
E-Folding Distance (km)	148.00	189.00	195.00	112.00
Life Time (hr)	4.50	7.50	7.20	4.20
Life Time- Lower Wind (hr)	8.60	13.80	12.40	7.30
Life Time- Upper Wind (hr)	3.10	5.20	5.10	2.90
Satellite Emission Rate (moles/s)	55.20	55.90	32.50	29.00
Sat NO <sub>x</sub> Emissions-1 - Lower (moles/s)	35.50	37.40	22.10	18.70
Sat NO <sub>x</sub> Emissions-1 - Upper (moles/s)	74.80	74.30	42.80	39.20
Sat NO <sub>x</sub> Emissions-2 - Lower (moles/s)	29.00	30.50	18.80	16.40
Sat NO <sub>x</sub> Emissions-2 - Upper (moles/s)	81.30	81.20	46.10	41.50
NAEI Emission Rate (moles/s)	30.90	30.90	30.90	12.90

Source Name	Birmingham	Birmingham	Newcastle	Manchester
Longitude	-1.89	-1.89	-1.62	-2.25
Latitude	52.50	52.50	54.98	53.50
Lon Edge - West	-2.18	-2.18	-1.73	-2.47
Lon Edge - East	-1.72	-1.72	-1.40	-2.01
Lat Edge - South	52.35	52.35	54.92	53.37
Lat Edge - North	52.66	52.66	55.02	53.60
Wind Speed Average (m/s)	5.80	9.10	10.50	5.60
Wind Speed Standard Deviation (m/s)	2.60	4.70	4.30	2.50
Wind Direction	N	S	W	N
E-Folding Distance (km)	184.00	91.00	297.00	152.00
Life Time (hr)	8.70	2.80	7.90	7.50
Life Time- Lower Wind (hr)	15.80	5.80	13.60	13.60
Life Time- Upper Wind (hr)	6.00	1.80	5.60	5.20
Satellite Emission Rate (moles/s)	12.20	25.20	1.70	20.5
Sat NO <sub>x</sub> Emissions-1 - Lower (moles/s)	8.10	16.70	0.80	13.00
Sat NO <sub>x</sub> Emissions-1 - Upper (moles/s)	16.40	33.70	2.60	28.10
Sat NO <sub>x</sub> Emissions-2 - Lower (moles/s)	6.80	12.20	1.00	11.30
Sat NO <sub>x</sub> Emissions-2 - Upper (moles/s)	17.70	38.20	2.40	29.80
NAEI Emission Rate (moles/s)	12.90	12.90	3.10	10.00

<b>Source Name</b>	Belfast	Edinburgh	Norwich	Cardiff
<b>Longitude</b>	-5.93	-3.19	1.29	-3.18
<b>Latitude</b>	54.61	55.96	52.63	51.49
<b>Lon Edge - West</b>	-6.00	-3.32	1.20	-3.36
<b>Lon Edge - East</b>	-5.84	-3.10	1.38	-3.10
<b>Lat Edge - South</b>	54.55	55.89	52.60	51.45
<b>Lat Edge - North</b>	54.70	55.98	52.69	51.55
<b>Wind Speed Average (m/s)</b>	8.30	10.10	10.30	5.30
<b>Wind Speed Standard Deviation (m/s)</b>	4.10	4.20	4.8	2.50
<b>Wind Direction</b>	E	W	W	N
<b>E-Folding Distance (km)</b>	87.00	262.00	214.00	86.00
<b>Life Time (hr)</b>	2.90	7.20	5.80	4.50
<b>Life Time- Lower Wind (hr)</b>	5.80	12.20	11.00	8.60
<b>Life Time- Upper Wind (hr)</b>	1.90	5.10	3.90	3.00
<b>Satellite Emission Rate (moles/s)</b>	3.40	1.90	2.40	2.50
<b>Sat NOx Emissions-1 - Lower (moles/s)</b>	2.10	0.80	1.30	1.50
<b>Sat NOx Emissions-1 - Upper (moles/s)</b>	4.80	3.10	3.40	3.50
<b>Sat NOx Emissions-2 - Lower (moles/s)</b>	1.70	1.10	1.20	1.30
<b>Sat NOx Emissions-2 - Upper (moles/s)</b>	5.20	2.70	3.50	3.70
<b>NAEI Emission Rate (moles/s)</b>	1.60	1.50	1.00	2.20

727

<b>Source Name</b>	Leeds	Bristol
<b>Longitude</b>	-1.55	-2.59
<b>Latitude</b>	53.80	51.46
<b>Lon Edge - West</b>	-1.69	-2.74
<b>Lon Edge - East</b>	-1.44	-2.47
<b>Lat Edge - South</b>	53.74	51.40
<b>Lat Edge - North</b>	53.86	51.55
<b>Wind Speed Average (m/s)</b>	8.70	7.20
<b>Wind Speed Standard Deviation (m/s)</b>	4.50	3.40
<b>Wind Direction</b>	S	E
<b>E-Folding Distance (km)</b>	207.00	123.00
<b>Life Time (hr)</b>	6.60	4.70
<b>Life Time- Lower Wind (hr)</b>	13.90	8.90
<b>Life Time- Upper Wind (hr)</b>	4.30	3.20
<b>Satellite Emission Rate (moles/s)</b>	5.70	3.80
<b>Sat NOx Emissions-1 - Lower (moles/s)</b>	3.70	2.50
<b>Sat NOx Emissions-1 - Upper (moles/s)</b>	7.60	5.10
<b>Sat NOx Emissions-2 - Lower (moles/s)</b>	2.70	2.00
<b>Sat NOx Emissions-2 - Upper (moles/s)</b>	8.60	5.50
<b>NAEI Emission Rate (moles/s)</b>	3.40	3.50

728

729